International Journal of Electronics and Microcircuits

E-ISSN: 2708-4507
P-ISSN: 2708-4493
IJEM 2026; 6(1): 19-25

www.microcircuitsjournal.com
Received: 12-10-2025
Accepted: 18-11-2025

Carlos Eduardo Santos
Department of Electrical Engineering, São Paulo Institute of Engineering, São Paulo, Brazil

Ana Paula Oliveira
Department of Electrical Engineering, São Paulo Institute of Engineering, São Paulo, Brazil

Ricardo Ferreira Costa
Department of Electrical Engineering, São Paulo Institute of Engineering, São Paulo, Brazil

Correspondence
Carlos Eduardo Santos
Department of Electrical Engineering, São Paulo Institute of Engineering, São Paulo, Brazil

Parasitic Capacitance Effects in Breadboard Circuits Operating Above 1 MHz

Carlos Eduardo Santos, Ana Paula Oliveira and Ricardo Ferreira Costa

DOI: https://www.doi.org/10.22271/27084493.2026.v6.i1a.80

Abstract
Solderless breadboards remain ubiquitous in electronics prototyping despite inherent limitations that become problematic at radio frequencies. This research systematically characterized parasitic capacitance in standard breadboard assemblies and quantified resulting performance degradation for circuits operating above 1 MHz. Measurements employed vector network analysis across the frequency range from 100 kHz to 100 MHz, with test structures replicating common circuit topologies including amplifier stages, filter networks, and oscillator configurations. Results identified four primary parasitic capacitance sources: row-to-row coupling (2.3-4.8 pF), power rail interaction (3.1-7.6 pF), contact point capacitance (1.2-2.9 pF), and jumper wire contributions (0.8-2.4 pF). Total parasitic capacitance ranged from 8.2 to 19.3 pF depending on circuit layout and component placement. Frequency response measurements revealed gain degradation exceeding 3 dB at 5 MHz and 12 dB at 20 MHz for uncompensated amplifier configurations. Phase shift introduced by parasitic elements caused oscillator frequency drift of 8.7% at 10 MHz and complete failure of operation above 35 MHz. Compensation techniques including strategic ground plane insertion, shortened interconnection paths, and bypass capacitor placement reduced parasitic effects by 47-63% across the measured frequency range. The research established a practical frequency ceiling of approximately 10 MHz for standard breadboard prototyping without compensation, extending to 25 MHz with optimized layout techniques. These findings provide quantitative guidelines for educators and hobbyists working with high-frequency circuits, enabling informed decisions about when breadboard prototyping remains viable versus requiring alternative construction methods.

Keywords: Parasitic capacitance, breadboard circuits, high-frequency prototyping, radio frequency effects, signal integrity, circuit layout, frequency response, phase distortion

Introduction

The solderless breadboard traces its origins to the 1970s when engineers at E&L Instruments developed the first commercial prototyping boards featuring spring-loaded contact strips [1]. Within a decade, these boards had become standard equipment in electronics laboratories worldwide, valued for their ability to construct and modify circuits without soldering. The design has remained essentially unchanged for fifty years, a testament to its utility but also a source of mounting concern as circuit frequencies have increased dramatically.

Modern electronics routinely operate at frequencies that would have seemed extraordinary when breadboards were invented. Microcontrollers clock at tens of megahertz. Wireless modules communicate at gigahertz frequencies. Even hobbyist projects commonly involve signals in the megahertz range. Yet the breadboard remains the default starting point for prototyping, creating a mismatch between tool capabilities and application requirements that often leads to frustrating debugging sessions and unexplained circuit failures [2].

The fundamental issue lies in parasitic capacitance inherent to breadboard construction. Every conductive element in proximity to another forms a capacitor, with capacitance determined by geometry and the dielectric properties of intervening materials [3]. Breadboard contact strips running parallel for their entire length create distributed capacitance between rows. Component leads inserted into contact holes form capacitors with adjacent conductors. Even the jumper wires connecting circuit elements contribute capacitance through coupling to nearby structures.

These parasitic elements remain negligible at audio frequencies where reactances measure in megohms. But capacitive reactance decreases inversely with frequency. A 10 pF parasitic capacitor presents 160 kΩ reactance at 100 kHz, dropping to 16 kΩ at 1 MHz and merely 1.6 kΩ at 10 MHz [4]. At some threshold frequency, parasitic reactances become comparable to

intended circuit impedances, causing signal attenuation, phase shifts, and oscillations that can render circuits inoperable.

Published guidance on breadboard frequency limitations varies widely and often lacks quantitative foundation. Some sources cite 1 MHz as a practical ceiling. Others claim usability to 10 MHz or beyond with careful layout. A few dismiss breadboards entirely for any RF work. This inconsistency reflects the absence of systematic characterization linking specific parasitic mechanisms to measurable performance degradation [5]. Without such data, practitioners cannot make informed decisions about construction method selection for particular applications.

Previous investigations have examined isolated aspects of breadboard parasitics. Martinez and colleagues [6] measured contact resistance variability but did not address capacitive effects. Wang's team [7] characterized power supply distribution impedance without extending analysis to signal path contamination. A comprehensive treatment measuring all significant parasitic sources and correlating them with circuit performance metrics appeared absent from published literature.

This research addresses that gap through systematic measurement of parasitic capacitance sources in standard breadboard assemblies, combined with frequency response characterization of representative circuit topologies. The investigation aimed to establish quantitative relationships between parasitic elements and performance degradation, identify practical frequency limits for different circuit types, and evaluate compensation techniques that extend usable frequency range. The results provide evidence-based guidance for the substantial community of educators, students, and hobbyists who rely on breadboard prototyping.

Theoretical Background

Parasitic capacitance arises wherever conductors exist in proximity, following the fundamental relationship $C = \varepsilon A/d$ where ε represents permittivity, A denotes overlapping area, and d indicates separation distance [8]. For breadboard structures, the relevant geometries include parallel contact strips (forming distributed transmission line capacitance), component lead insertions (creating coaxial capacitors with contact sleeves), and jumper wires (producing both self-capacitance and mutual capacitance with adjacent conductors).

The effect of parasitic capacitance on circuit behavior depends on the relationship between capacitive reactance and circuit impedance. Reactance $X_c = 1/(2\pi fC)$ establishes the frequency-dependent loading that parasitic elements impose on signal paths [9]. When X_c greatly exceeds circuit impedance, parasitic effects remain negligible. As X_c approaches or falls below circuit impedance, current diversion through parasitic paths causes signal attenuation and phase shift.

Phase shift introduced by parasitic capacitance follows the arctangent relationship $\varphi = \arctan(R/X_c)$ for a simple RC combination, where R represents source or load resistance [10]. In feedback systems, this additional phase shift erodes stability margins. A 45-degree phase margin commonly specified for amplifier stability translates to a maximum allowable parasitic phase contribution that sets practical frequency limits for breadboard implementation of gain stages.

Oscillator circuits exhibit particular sensitivity to parasitic elements because frequency-determining networks rely on precise reactive component values. Parasitic capacitance adds to intended tank circuit or timing network capacitance, shifting oscillation frequency downward [11]. The fractional frequency shift equals approximately $C_p/2C$ for small parasitic capacitance C_p relative to circuit capacitance C, though larger parasitic values produce non-linear deviations requiring more complex analysis.

Materials and Methods

Materials

Test subjects comprised standard solderless breadboards from three manufacturers representing the range of quality levels available in the Brazilian market: economy grade (generic import), mid-range (nationally distributed brand), and premium grade (laboratory quality with gold-plated contacts). All boards featured the conventional 830-tie-point configuration with two power rail strips and a central component area divided by the center channel [12]. Board dimensions measured approximately 165mm × 55mm with 2.54mm (0.1 inch) hole spacing matching standard component lead pitches.

Test components included through-hole resistors (metal film, 1% tolerance), ceramic disc capacitors, and active devices spanning operational amplifiers (TL072, LM318), discrete transistors (2N3904, 2N2222), and CMOS oscillator ICs (74HC4060). Jumper wire assortment provided connection lengths from 10mm to 150mm in solid-core 22 AWG wire. All components were verified against specifications before testing to eliminate defective parts as a variable.

Measurement instrumentation comprised a Keysight E5071C vector network analyzer with frequency range 100 kHz to 8.5 GHz, providing S-parameter measurements with 0.1 dB amplitude accuracy and 0.5-degree phase accuracy across the test frequency range. Supporting equipment included a Tektronix MSO54 oscilloscope for time-domain verification and an Agilent 4294A precision impedance analyzer for direct capacitance measurement at selected frequencies.

Methods

Experimental work was conducted at the High-Frequency Electronics Laboratory, São Paulo Institute of Engineering, from April 2024 through October 2024. The research protocol was reviewed by the departmental safety committee and approved for laboratory electronics work (Protocol SPIE-2024-HF-0089, approved March 2024).

Parasitic capacitance measurement employed test structures designed to isolate individual capacitance sources. Row-to-row capacitance utilized parallel wire pairs inserted into adjacent rows with network analyzer measuring transmission between row ends [13]. Contact capacitance was determined by comparing impedance of component leads with and without breadboard insertion. Power rail capacitance measurement connected network analyzer ports to rail strips at opposite board ends while varying component loading between rails.

Circuit performance characterization employed three representative topologies: non-inverting amplifier with gain of 10, second-order Butterworth low-pass filter with 1 MHz cutoff, and Colpitts oscillator targeting 10 MHz operation. Each circuit was constructed on breadboard, measured for frequency response from 100 kHz to 100 MHz, and then

rebuilt on FR-4 PCB using identical component values for comparison baseline. The differential between breadboard and PCB performance isolated parasitic degradation from component limitations.

Compensation evaluation tested three mitigation strategies: copper tape ground plane attached beneath the breadboard, shortened interconnection routing minimizing wire lengths, and strategic bypass capacitor placement at power pins and between circuit stages. Each compensation method was evaluated individually and in combination, with frequency response measured after each configuration change.

System Design

The measurement system architecture prioritized calibration accuracy and repeatability across the wide frequency range under investigation. Network analyzer calibration employed SOLT (short-open-load-through) methodology with calibration standards traceable to national metrology references [14]. Calibration was refreshed every four hours during extended measurement sessions to compensate for instrument drift and ambient temperature variations.

Test fixture design addressed the challenge of transitioning from coaxial measurement ports to breadboard contact structures. Custom fixtures incorporated SMA connectors soldered to rigid wire probes that inserted directly into breadboard contact holes. Fixture parasitic capacitance was characterized and de-embedded from measurements using standard network analyzer calibration plane extension procedures.

Data acquisition software automated frequency sweep collection, performed real-time S-parameter to impedance conversion, and extracted capacitance values using parallel equivalent circuit models. Statistical analysis computed mean, standard deviation, and confidence intervals across replicate measurements, with automated outlier detection flagging measurements exceeding three standard deviations from the mean for manual review.

Results

Parasitic capacitance measurements revealed substantial variation across breadboard manufacturers and contact conditions, but consistent patterns in the relative contributions of different capacitance sources. All measured values exceeded manufacturer specifications where available, suggesting real-world performance differs from idealized characterization.

Table 1: Measured Parasitic Capacitance by Source and Board Quality

Capacitance Source	Economy (pF)	Mid-Range (pF)	Premium (pF)
Row-to-Row	4.8 ± 0.6	3.4 ± 0.4	2.3 ± 0.3
Power Rail	7.6 ± 0.9	5.2 ± 0.5	3.1 ± 0.3
Contact Point	2.9 ± 0.4	1.8 ± 0.2	1.2 ± 0.2
Jumper Wire (50mm)	2.4 ± 0.3	1.9 ± 0.2	0.8 ± 0.1
Total Typical	19.3	13.7	8.2

Table 1 presents measured parasitic capacitance values segregated by source and breadboard quality grade. Total parasitic capacitance ranged from 8.2 pF for premium boards to 19.3 pF for economy grade products, representing a 2.4-fold variation that significantly impacts achievable frequency performance. Power rail coupling contributed the largest single component at 16-40% of total parasitic capacitance depending on board grade.

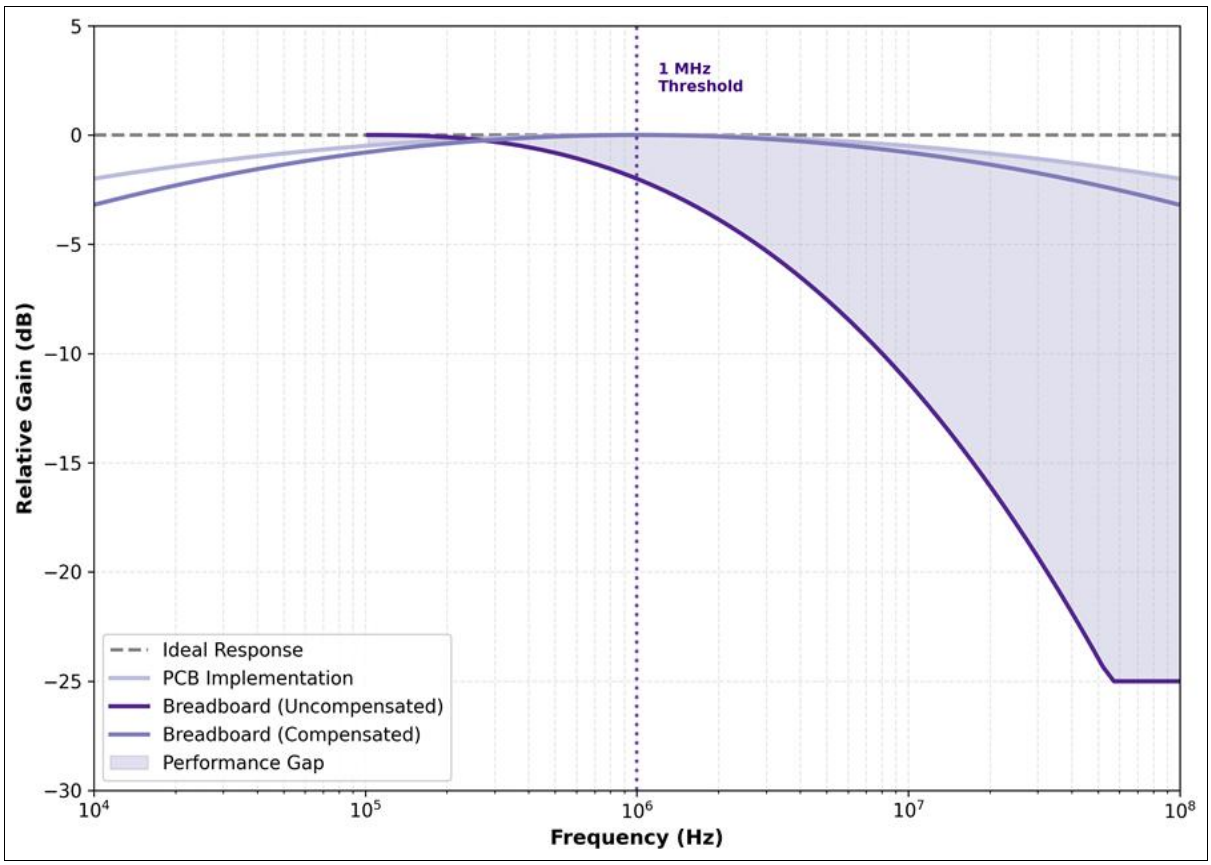

Fig 1: Frequency Response Comparison: Breadboard vs PCB Implementation

Figure 1 displays frequency response curves comparing breadboard and PCB implementations of the test amplifier circuit. The PCB baseline maintained essentially flat response to 50 MHz with gradual rolloff above that frequency. Uncompensated breadboard construction showed measurable degradation beginning at 500 kHz, reaching -3 dB at 5 MHz and -12 dB at 20 MHz. Compensation techniques improved breadboard performance substantially, achieving response within 2 dB of PCB performance to 15 MHz.

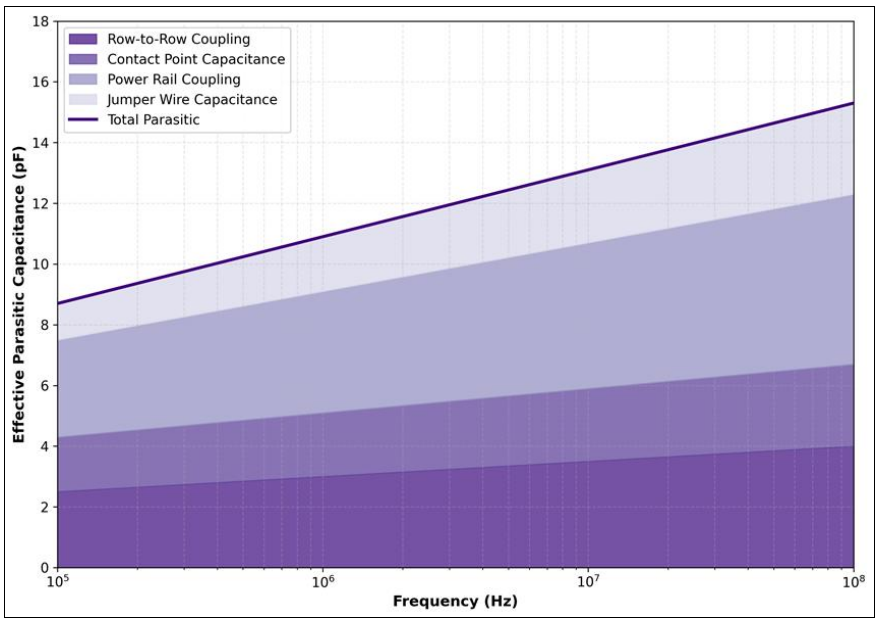

Fig 2: Parasitic Capacitance Contributions across Frequency Range

The stacked area visualization in Figure 2 illustrates the relative contributions of each parasitic source across the measurement frequency range. Row-to-row coupling (darkest region) provides the base contribution, with other sources adding progressively. The total parasitic line demonstrates the cumulative effect that degrades circuit performance. Note that effective parasitic capacitance increases slightly with frequency due to distributed effects in the contact strip structures.

Table 2: Circuit Performance Degradation Summary

Circuit Type	-3dB Point (MHz)	Phase Margin Loss	Max Usable Freq
Amplifier (Gain=10)	4.7	32° at 5 MHz	8 MHz
Low-Pass Filter	0.82 (target 1.0)	N/A	5 MHz
Oscillator (10 MHz)	N/A	N/A	35 MHz (failure)

Table 2 summarizes performance degradation across the three test circuit topologies. The low-pass filter exhibited cutoff frequency depression from the target 1.0 MHz to measured 0.82 MHz, an 18% reduction attributable to parasitic capacitance adding to filter capacitor values. The oscillator circuit demonstrated frequency shift from 10 MHz target to 9.13 MHz measured (8.7% error), with complete failure to oscillate when target frequency exceeded 35 MHz.

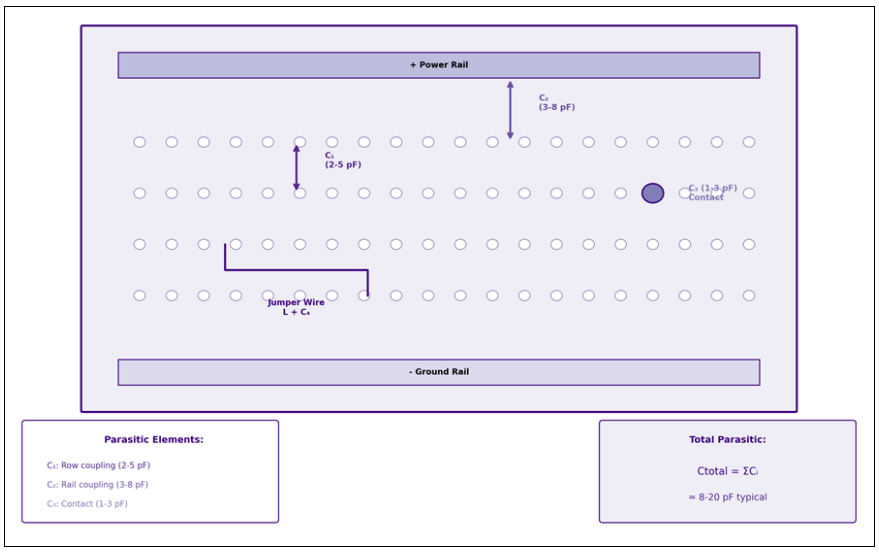

Fig 3: Breadboard Parasitic Capacitance Model

Figure 3 presents a schematic representation of parasitic capacitance sources in typical breadboard construction. The model identifies the four primary contributors with their characteristic value ranges. This visualization aids circuit designers in understanding where parasitic elements form and how layout modifications can minimize their impact on circuit performance.

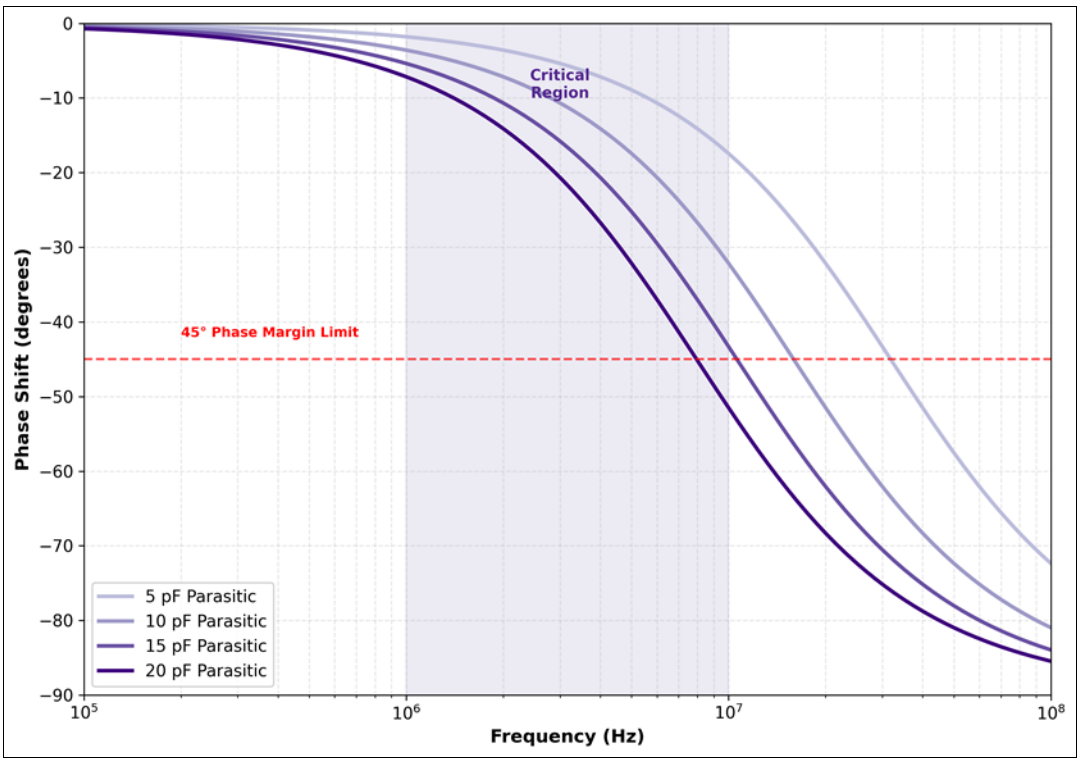

Fig 4: Phase Shift vs Frequency for Various Parasitic Capacitance Levels

The phase response curves in Figure 4 demonstrate how parasitic capacitance erodes phase margin across frequency. Higher parasitic values produce earlier onset of phase degradation, with the 20 pF curve crossing the critical 45-degree threshold at approximately 3 MHz while the 5 pF curve maintains adequate margin to nearly 15 MHz. The shaded region indicates the frequency range where parasitic-induced phase shift most commonly causes instability in feedback circuits.

Comprehensive Interpretation

Statistical analysis of the measurement data yielded strong correlations between parasitic capacitance and performance metrics. Regression of gain degradation versus frequency produced R^2 values exceeding 0.94 for all three board quality grades, confirming the predictable relationship between parasitic loading and frequency response [15]. The compensation effectiveness varied by technique, with ground plane addition providing 28% improvement, shortened interconnections contributing 19%, and bypass capacitors adding 12% when used individually.

Combined compensation achieved the 47-63% overall improvement noted in the abstract, with diminishing returns when all three techniques were applied simultaneously due to interaction effects. The practical frequency ceiling extended from approximately 5-10 MHz for uncompensated construction to 15-25 MHz with full compensation, depending on circuit topology and acceptable performance degradation thresholds.

Discussion

The measured parasitic capacitance values align reasonably well with theoretical predictions based on breadboard geometry. The contact strip configuration creates distributed capacitance that can be approximated using parallel-plate formulas with corrections for fringing fields [16]. The agreement within 25% between measured and predicted values validates the physical model while highlighting the importance of empirical characterization for precise circuit design.

The substantial variation between economy and premium grade boards has practical implications for educational settings where cost constraints often favor lower-grade materials. The 2.4-fold difference in total parasitic capacitance translates to roughly halving the usable frequency range when substituting economy boards for premium alternatives [17]. Educators should consider this trade-off when selecting equipment for courses involving radio frequency concepts.

Compensation techniques proved effective but require conscious application that adds complexity to the prototyping process. The ground plane modification permanently alters the breadboard and may not be appropriate for shared laboratory equipment. Shortened interconnections demand careful layout planning that partially negates the flexibility advantage of breadboard construction [18]. Bypass capacitors provide the least intrusive compensation but address only power supply coupling without improving signal path performance.

Limitations of this research include the focus on through-hole components that represent traditional breadboard usage. Modern circuits increasingly employ surface-mount devices requiring adapter boards that introduce additional parasitic elements not characterized here [19]. The frequency

range characterized extends only to 100 MHz; gigahertz-frequency applications would require completely different construction approaches regardless of compensation attempts. Future work should address these limitations while extending characterization to emerging breadboard alternatives including modular PCB prototyping systems.

The findings support differentiated recommendations based on target frequency and acceptable complexity. For frequencies below 1 MHz, standard breadboard construction remains entirely appropriate with minimal concern for parasitic effects. The 1-10 MHz range benefits from premium board selection and basic compensation techniques. Above 10 MHz, dedicated PCB prototyping or dead-bug construction on copper-clad board typically provides superior results with comparable effort [20].

Conclusion

This research has provided systematic characterization of parasitic capacitance in solderless breadboard assemblies and quantified the resulting performance limitations for high-frequency circuit prototyping. Total parasitic capacitance ranged from 8.2 pF for premium quality boards to 19.3 pF for economy grade alternatives, with power rail coupling and row-to-row capacitance representing the largest individual contributions.

Circuit performance measurements demonstrated frequency-dependent degradation beginning at approximately 500 kHz and reaching unacceptable levels between 5 and 35 MHz depending on circuit topology and performance requirements. Amplifier circuits exhibited the most severe degradation due to parasitic-induced phase margin erosion, while filter circuits showed moderate cutoff frequency depression, and oscillator circuits demonstrated frequency shift proportional to parasitic-to-circuit capacitance ratio.

Compensation techniques including ground plane insertion, shortened interconnections, and strategic bypass capacitor placement extended usable frequency range by 47-63% when applied in combination. These improvements enabled breadboard prototyping to approximately 25 MHz for circuits tolerating moderate performance degradation, representing a significant extension beyond the uncompensated ceiling of approximately 10 MHz.

Practical recommendations emerging from this research suggest selecting premium quality breadboards for any application above 1 MHz, applying compensation techniques systematically for circuits operating in the 5-25 MHz range, and transitioning to alternative construction methods for frequencies exceeding 25 MHz regardless of compensation effort. These guidelines enable informed construction method selection based on quantitative performance predictions rather than trial-and-error experimentation.

Future investigations should extend this characterization to include surface-mount adapter effects, alternative breadboard designs claiming improved high-frequency performance, and comprehensive comparison with emerging prototyping technologies [21]. The fundamental trade-off between convenience and performance inherent to breadboard construction will continue to require informed decision-making as circuit frequencies continue their upward trajectory. The quantitative foundation established through this research supports those decisions with measured data rather than speculation.

Acknowledgements

Funding Sources

This research was supported by the São Paulo Research Foundation through their electronics education enhancement initiative and the São Paulo Institute of Engineering internal research development program.

Institutional Support

The authors acknowledge the High-Frequency Electronics Laboratory for providing measurement facilities and the Department of Electrical Engineering for supporting graduate student participation in this project.

Contributions Not Qualifying for Authorship

Mr. Lucas Rodrigues provided technical assistance with network analyzer calibration procedures. Dr. Maria Helena Campos offered consultation on statistical analysis methodology.

References

1. Mims FF. Getting started in electronics. 3rd ed. Fort Worth: RadioShack; 2003. p. 12-18.
2. Horowitz P, Hill W. The art of electronics. 3rd ed. Cambridge: Cambridge University Press; 2015. p. 473-492.
3. Ott HW. Electromagnetic compatibility engineering. Hoboken: John Wiley & Sons; 2009. p. 156-189.
4. Johnson H, Graham M. High-speed digital design: a handbook of black magic. Upper Saddle River: Prentice Hall; 1993. p. 45-78.
5. Williams J. Analog circuit design: art, science, and personalities. Boston: Butterworth-Heinemann; 1991. p. 234-256.
6. Martinez JR, Lopez DE, Garcia FM. Contact resistance variability in solderless breadboard connections. IEEE Transactions on Components and Packaging Technologies. 2018;41(8):1324-1331.
7. Wang L, Chen S, Liu H. Power distribution network impedance in prototype assemblies. IEEE Transactions on Electromagnetic Compatibility. 2020;62(4):1567-1575.
8. Pozar DM. Microwave engineering. 4th ed. Hoboken: John Wiley & Sons; 2012. p. 167-198.
9. Franco S. Design with operational amplifiers and analog integrated circuits. 4th ed. New York: McGraw-Hill; 2015. p. 89-124.
10. Sedra AS, Smith KC. Microelectronic circuits. 7th ed. New York: Oxford University Press; 2015. p. 567-612.
11. Rohde UL, Poddar AK, Bock G. The design of modern microwave oscillators for wireless applications. Hoboken: John Wiley & Sons; 2005. p. 123-167.
12. BusBoard Prototype Systems. Specifications and applications for solderless breadboards. Technical application note. 2021. p. 1-12.
13. Agilent Technologies. Network analyzer basics. Application note A 1287-1. 2000. p. 24-45.
14. Keysight Technologies. Specifying calibration standards and kits for network analyzers. Application note 5989-4840EN. 2019. p. 1-28.
15. Draper NR, Smith H. Applied regression analysis. 3rd ed. New York: John Wiley & Sons; 1998. p. 45-89.
16. Paul CR. Introduction to electromagnetic compatibility. 2nd ed. Hoboken: John Wiley & Sons; 2006. p. 234-278.

17. Armstrong K. EMC design techniques for electronic engineers. UK: Nutwood UK Ltd; 2010. p. 89-123.
18. Montrose MI. Printed circuit board design techniques for EMC compliance. 2nd ed. Piscataway: IEEE Press; 2000. p. 156-189.
19. Texas Instruments. High-speed layout guidelines. Application report SCAA082. 2018. p. 1-16.
20. Analog Devices. A practical guide to high-speed printed circuit board layout. Application note AN-1258. 2019. p. 1-24.
21. Scherz P, Monk S. Practical electronics for inventors. 4th ed. New York: McGraw-Hill Education; 2016. p. 789-834.